

Probing the Energetic Particle Environment near the Sun

D.J. McComas¹, E.R. Christian², C.M.S. Cohen³, A.C. Cummings³, A.J. Davis³, M.I. Desai^{4,5}, J. Giacalone⁶, M.E. Hill⁷, C.J. Joyce¹, S.M. Krimigis⁷, A.W. Labrador³, R.A. Leske³, O. Malandraki⁸, W.H. Matthaeus⁹, R.L. McNutt Jr.⁷, R.A. Mewaldt³, D.G. Mitchell⁷, A. Posner¹⁰, J.S. Rankin¹, E.C. Roelof⁷, N.A. Schwadron^{1,11}, E.C. Stone³, J.R. Szalay¹, M.E. Wiedenbeck¹², S.D. Bale^{13,14}, J.C. Kasper¹⁵, A.W. Case¹⁶, K.E. Korreck¹⁶, R.J. MacDowall², M. Pulupa¹³, M.L. Stevens¹⁶, A.P. Rouillard¹⁷

¹Department of Astrophysical Sciences, Princeton University, Princeton, NJ 08544, USA

²Goddard Space Flight Center, Greenbelt, MD 20771, USA

³California Institute of Technology, Pasadena, CA 91125, USA

⁴Southwest Research Institute, San Antonio, TX 78228, USA

⁵University of Texas at San Antonio, San Antonio, TX 78249, USA

⁶University of Arizona, Tucson, AZ 85721, USA

⁷Johns Hopkins University Applied Physics Laboratory, Laurel, MD 20723, USA

⁸National Observatory of Athens, IAASARS, Athens 15236 Greece

⁹University of Delaware, Newark, DE 19716, USA

¹⁰NASA HQ, Washington DC 20024, USA

¹¹University of New Hampshire, Durham, NH 03824, USA

¹²Jet Propulsion Laboratory, California Institute of Technology, Pasadena, CA 91109, USA

¹³University of California at Berkeley, Berkeley, CA 94720, USA

¹⁴The Blackett Laboratory Imperial College London, London, SW7 2AZ, UK

¹⁵University of Michigan, Ann Arbor, MI 48109, USA

¹⁶Smithsonian Astrophysical Observatory, Cambridge, MA 02138, USA

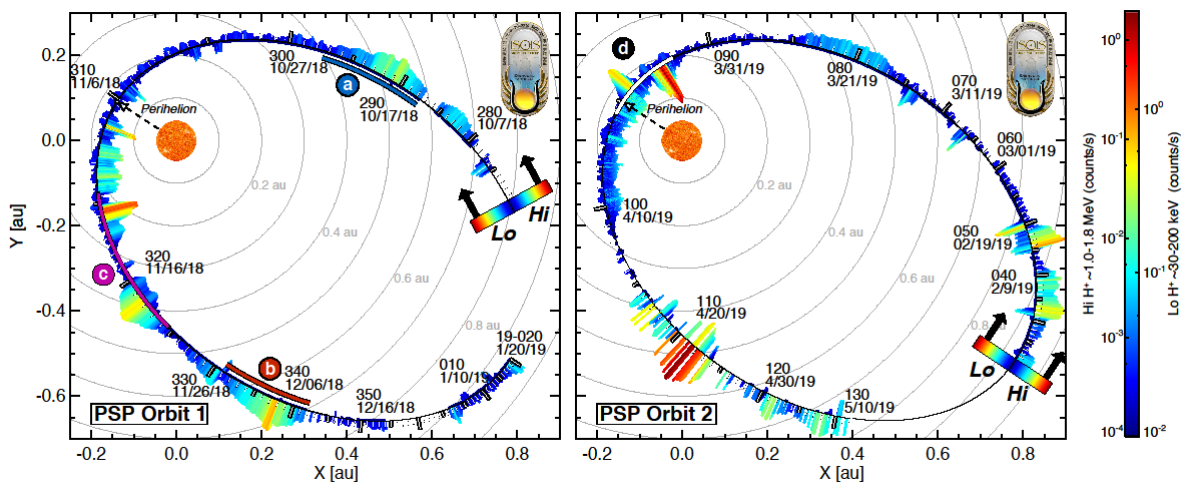
¹⁷CNRS, Toulouse Cedex 4, France

NASA's Parker Solar Probe mission¹ recently plunged through the inner heliosphere to perihelia at ~24 million km, much closer to the Sun than any prior human-made object. Prior studies further from the Sun indicate that solar energetic particles are accelerated from a few keV up to near-relativistic energies in at least two ways. First, magnetic reconnection associated with solar flares often produces smaller "impulsive" events typically enriched in electrons, ³He, and heavier ions². Second, large Coronal Mass Ejection-driven shocks and compressions moving through the corona and inner solar wind are associated with "gradual" events^{3,4} that predominantly generate 1-10 MeV protons. However, some events show aspects of both processes and there is no

35 bimodal distribution of the electron/proton ratio as expected for this simple picture⁵. Here we
 36 report the first observations of the near-Sun energetic particle radiation environment over PSP’s
 37 first two orbits. We find a great variety of different types of energetic particle events accelerated
 38 both locally and remotely, including by corotating interaction regions, impulsive events driven
 39 by acceleration near the Sun, and an event related to a Coronal Mass Ejection. These
 40 observations – so close to the Sun – provide critical information for investigating the near-Sun
 41 energization and transport of solar energetic particles. These processes were difficult, if not
 42 impossible, to resolve from prior observations owing to processing of energetic particle
 43 populations *en route* to more distant observing spacecraft⁶. Here we directly explore the physics
 44 of particle acceleration and transport in the context of various theories and models that have been
 45 developed over the past decades. Thus, this study marks a major milestone with humanity’s
 46 reconnaissance of the near-Sun environment and provides the first direct observations of the
 47 energetic particle radiation environment in the region just above the corona.

48 Onboard Parker Solar Probe (PSP), the Integrated Science Investigation of the Sun (ISOIS)
 49 instrument suite⁷ made groundbreaking measurements of solar energetic particles (SEPs). ISOIS
 50 comprises two Energetic Particle Instruments measuring higher (EPI-Hi or Hi) and lower (EPI-
 51 Lo or Lo) energy particles, with overlapping coverage⁷. Together this enables ISOIS to explore
 52 the near-Sun environment by measuring fluxes, energy spectra, anisotropy, and composition of
 53 suprathermal and energetic ions from ~ 0.02 –200 MeV/nucleon (nuc) and electrons from ~ 0.05 –
 54 6 MeV. Here, we examine this energetic particle environment in the context of *in situ* solar wind⁸
 55 and magnetic field⁹ conditions and surrounding density structures¹⁰ measured by other
 56 instruments aboard PSP.

57 Fig. 1 summarizes ISOIS observations of energetic particles over PSP’s first two orbits. Higher
 58 (1-2 MeV) and lower (30-200 keV) energy H^+ ion counts are plotted on the outside and inside of
 59 the orbital trajectory, respectively. Intensifications indicate energetic particle events, with some
 60 seen only at higher energies, some only at lower energies, and others simultaneously at both. Fig.
 61 1 indicates how rich the ISOIS observations are, with a broad array of different types of particle
 62 events at all distances.



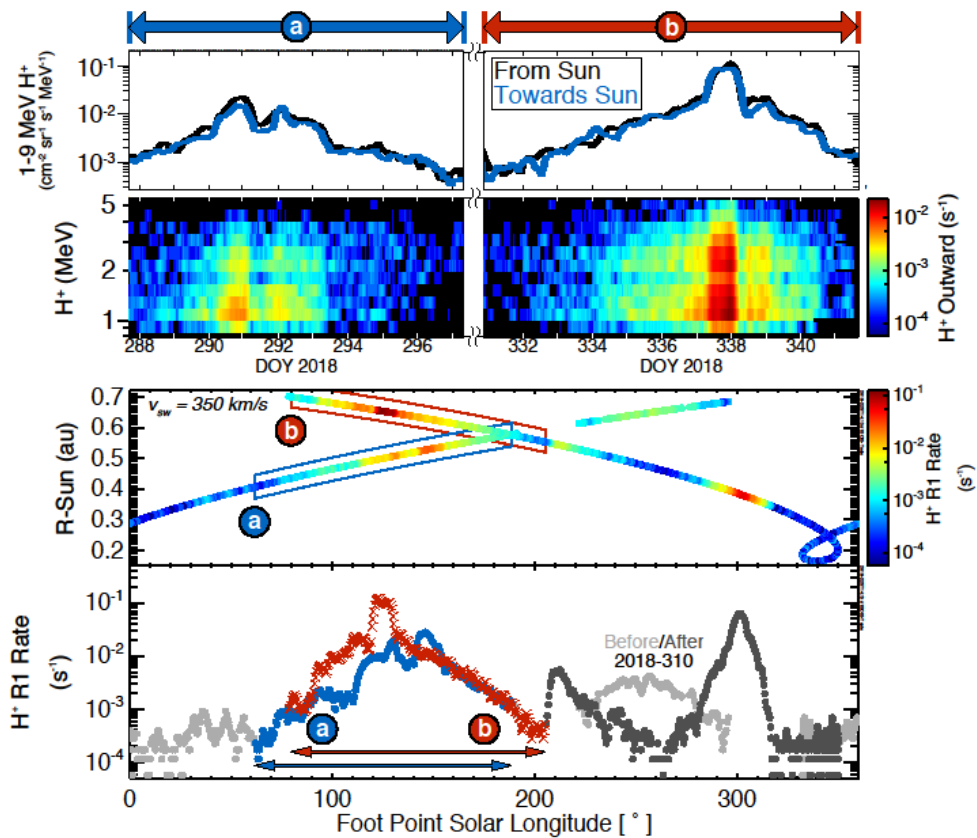
63
 64 Fig. 1: Summary of observations of energetic particles (primarily H^+) at lower energy (Lo: ~ 30 -
 65 200 keV, inside orbital track) and higher energy (Hi: ~ 1 -2 MeV, outside orbital track) from
 66 PSP’s first two orbits; intervals without data are indicated by the grey orbital track. Particle

67 intensity is indicated by both color and length of the bars. We identify Intervals **a-d** for detailed
 68 study.

69 The first large intensification occurred at higher energies with PSP inbound in Orbit 1 (Interval
 70 **a**, 2018-287 18:00 to 2018-297 08:20 UT) at ~ 0.5 au. While not obvious from Fig. 1, this is a
 71 corotational event also seen when PSP was outbound at ~ 0.65 au (Interval **b**, 2018-330 23:20 to
 72 2018-341 15:00 UT). Corotating Interaction Regions (CIRs) form as faster solar wind piles up
 73 behind slower wind, forming a compression^{11,12}. Because these faster solar wind streams emanate
 74 from coronal holes at the Sun, CIRs map to nearly fixed solar longitudes.

75 Fig. 2 shows Intervals **a** and **b** as a function of solar surface “foot point” longitude, calculated for
 76 a nominal Parker Spiral with a fixed solar wind speed of 350 km s^{-1} . This calculation combines
 77 the rotation of the Sun and spacecraft location to show that both events arise from the same,
 78 single CIR structure. These events are “dispersionless,” with all ions arriving at roughly the same
 79 time and fluctuations in intensity consistent across ion speeds. Such events indicate that PSP
 80 passed across magnetic flux tubes that were already filled with high-energy ($>1 \text{ MeV}$) particles
 81 that move quickly along the field. Intensities of sunward and anti-sunward moving particles in
 82 Intervals **a** and **b** were similar (top panels), consistent with a corotating structure that traps
 83 particles between a source further out than the spacecraft and the increasing magnetic field
 84 strength closer to the Sun. The particle acceleration probably occurs at reverse shocks, which
 85 typically form beyond ~ 2 au from compressions in such CIRs.

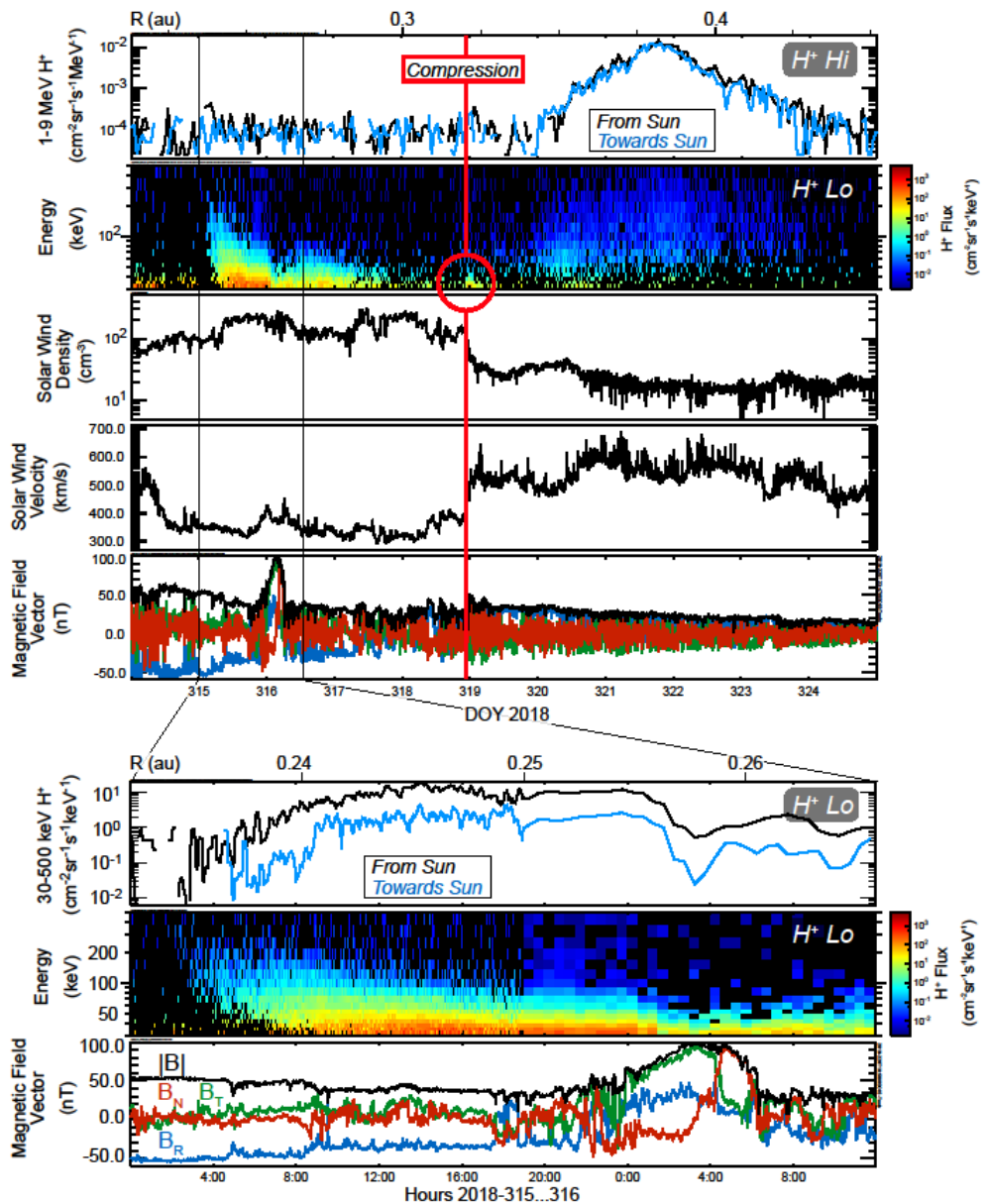
86



87

88 Fig. 2: Corotating ion event seen in Intervals **a** (blue) and **b** (red) versus time (top) and as a
 89 function of magnetic foot-point in Carrington longitude for a nominal 350 km s^{-1} solar wind
 90 speed (bottom panels).

91 The inbound leg toward perihelion 1 was extremely quiet from $\sim 0.4 \text{ au}$, providing an ideal
 92 opportunity for other PSP instruments to observe very quiet solar wind conditions with
 93 essentially no SEP-produced penetrating backgrounds. ISOIS began to observe lower energy
 94 SEPs starting just before and increasing after perihelion 1. Fig. 3 shows the events in Interval **c**,
 95 including low energy ions ahead of a CME, the passage of a compression wave after it, and a
 96 subsequent higher energy particle event.



98 *Fig. 3: Time series (top five panels) of primarily protons at >1 MeV and ~30-500 keV, density*
99 *and radial speed¹³ and magnetic field vector and magnitude¹⁴ over Interval c. The bottom three*
100 *panels expand the dispersive SEP event and CME.*

101 ISOIS observations show an SEP event starting early on 2018-315 and extending to about when
102 the CME arrived at PSP on 2018-316. Particle anisotropies (third panel from bottom)
103 demonstrate that these particles are streaming outward from the Sun. The faster particles arrive
104 first, characteristic of a “dispersive SEP event,” (second panel from bottom) with the differing
105 arrival times giving an estimate of the distance along the magnetic field back to their acceleration
106 source. For the time/energy slope in Fig. 3, we estimate a path length³ longer than the Parker
107 Spiral from PSP at ~0.25 au, which might be explained by a longer path length associated with
108 magnetic field “switchbacks” observed by PSP *in situ*¹⁴.

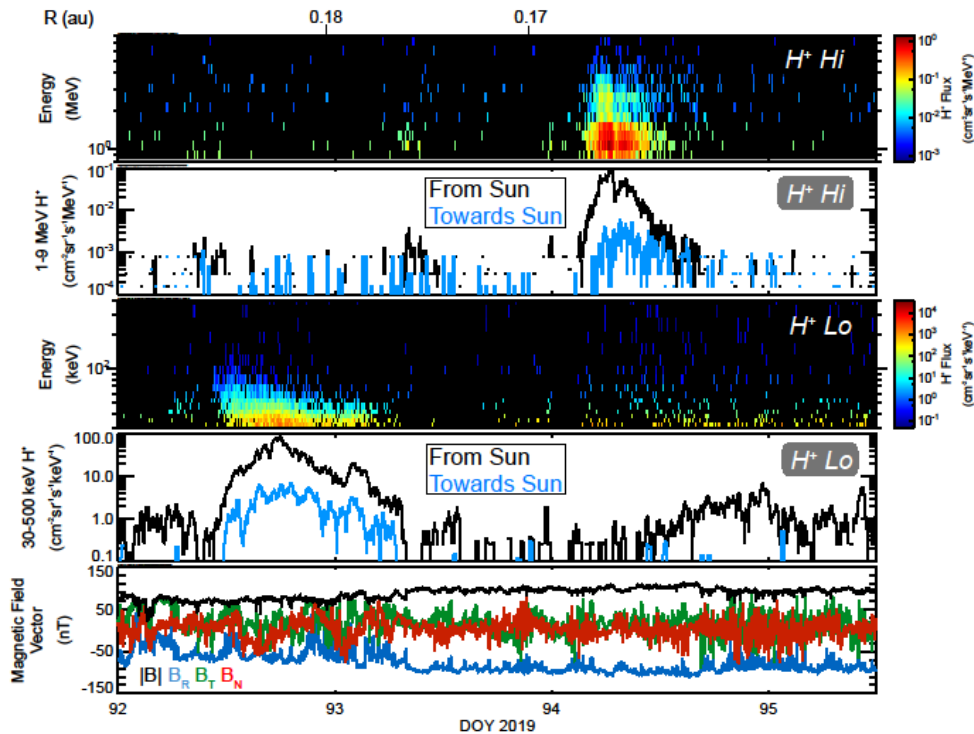
109 Solar observations from the white light coronagraph on the “A” spacecraft of NASA’s Solar
110 Terrestrial Relations Observatory (STEREO-A) indicate that the SEP-associated CME started
111 lifting off from the Sun on 2018-314 at ~18 UT (Extended Data Fig. 1). Derivation of the CME
112 speed from STEREO-A imaging (Extended Data Fig. 2) reveals that the CME was moving
113 slowly (<400 km/s) from the Sun to PSP, very similar to the surrounding solar wind speed. By
114 propagating this CME flux rope at a constant speed of 380 km s⁻¹ from near the sun to PSP, we
115 find good agreement with the *in situ* magnetic field observations. Preliminary analysis of this
116 event using shock-modeling techniques¹⁵ suggests that there was likely no shock on field lines
117 well connected to PSP. However, a quasi-perpendicular sub-critical shock (Mach number <3)
118 could have formed over an extended region of the flux rope and perhaps accelerated the protons
119 measured by PSP (A. Kouloumvakos, private communication). This energetic particle event was
120 not seen at any of the 1 au spacecraft, so such small events may only be observable close to the
121 Sun and therefore much more common than previously thought.

122 At the end of 2018-318, the solar wind speed increased from ~300 to ~500 km s⁻¹ [13], indicative
123 of a strong dynamic pressure wave in the solar wind. ISOIS observes a small enhancement in
124 very low energy particles (<50 keV) as this compressional wave passes. This event is the first
125 direct observation of local energization in the ISOIS observations. Shocks are not required for
126 particle acceleration¹⁶ and plasma compressions can accelerate particles provided the particles
127 are able to propagate across, but remain close to the compression¹⁷.

128 The large, two-step increase in speed shows that this wave is well on its way to steepening into a
129 forward/reverse shock pair, which most likely accelerates the higher (>1 MeV) energy particles
130 observed from 2018-320 to 2018-324. This is not a CIR as in Intervals **a** and **b**, as it has a much
131 narrower range of foot point longitudes (see enhancement at ~300° in Figure 2) and does not
132 recur, but instead indicates the interaction of a single fast solar wind stream, possibly associated
133 with or even magnetically opened by the preceding CME. In any case, as with CIR-associated
134 particle events, the particle isotropy indicates that these ions are trapped on flux tubes, likely
135 with a source beyond PSP. In fact, while the second event was seen ~1-6 days after the passage
136 of the compression at PSP, the pressure front had expanded outward to heliocentric distances of
137 ~0.6-2 au, where it likely formed the shocks.

138 Very near perihelion (~35 Solar Radii, R_☉) on PSP Orbit 2 (Interval **d**), ISOIS observed a unique
139 pair of SEP events (Fig. 4). As PSP is nearly co-rotational with the Sun near perihelion, the two
140 events are magnetically connected to a common solar source <5° apart in longitude. First, on
141 2019-092 there was a low-energy dispersive event, probably associated with an impulsive source

142 in the low corona. Two days later, on 2019-094, there was a quite different type of impulsive
 143 event, marked by a substantial enhancement of >1 MeV ions. Both events exhibit strong,
 144 persistent magnetic-field-aligned ions streaming away from the Sun.



145
 146 *Fig. 4: Two impulsive SEP events (Interval **d**) near PSP’s second perihelion ($<40 R_{\odot}$) at higher*
 147 *energies (top two panels) and lower energies (third and fourth panels), compared to the*
 148 *magnetic field (bottom).*

149 The first event, starting on 2019-092, may be associated with disturbances in EUV images from
 150 STEREO-A in the vicinity of active region AR2738, as well as multiple type-III radio bursts by
 151 both STEREO-A and PSP/FIELDS¹⁴. This small active region was $\sim 70^{\circ}$ off the nominal
 152 magnetic connection of PSP to the Sun. The fluxes of high-energy protons are near background,
 153 but we observed a statistically significant number of heavy, high-energy, ions and at low
 154 energies (~ 30 keV/nuc). He/H is ~ 20 times higher than the event on 2019-094, and the O and Fe
 155 abundances are even more enhanced. These results suggest that this may be a “Z-rich” event¹⁸;
 156 such events are relatively rare at 1 AU.

157 The second SEP event, on 2019-094 also exhibits velocity dispersion and outward streaming, but
 158 has many fewer ions <1 MeV and a significant increase at >1 MeV. As with 2019-092, there is
 159 potentially related radio and EUV activity in AR2738. However, the heavy ion abundances were
 160 similar to more typical solar energetic particle events. The magnetic field observed at PSP
 161 (bottom panel) between the two events was stronger and significantly smoother than before or
 162 after, indicating that this was likely a single, lower β (particle pressure/magnetic pressure)
 163 magnetic structure connecting the two events. Further, these observations indicate that processes

164 inside 0.17 AU, as suggested by early multi-spacecraft studies in Solar Cycle 20, as well as later
165 Helios and STEREO studies^{19,20,21,22}, enable fast, direct access of SEPs to a wide range of solar
166 longitudes. Later studies that combined in-situ data with solar source region observations showed
167 that the smaller, longitudinally distributed SEP events are associated with multiple jet-like
168 coronal emissions^{23,24} close to the source region as well as with more spatially extended
169 eruptions²⁵.

170 ISOIS observed a surprisingly rich array of energetic particle phenomena during PSP's first two
171 orbits. Several of these events were not observed by 1 au spacecraft, so small events, only
172 observable close to the Sun, may be much more common than previously thought. With these
173 new data, we are well on the way to resolving the fundamental questions of the origin,
174 acceleration, and transport of SEPs into the heliosphere. Over the next five years, as we head
175 toward solar maximum, PSP will orbit progressively closer to the Sun, ultimately extending our
176 exploration of these critical processes down to inside 10 R_⊙.

177

178 **References and Notes**

- 179 1. Fox, N. J. et al. The Solar Probe Plus mission: Humanity's first visit to our star. *Space*
180 *Science Reviews* 204, 7-48 (2016).
- 181 2. Mason, G. M. ³He-Rich Solar Energetic Particle Events. *Space Science Reviews* 130,
182 231-242 (2007).
- 183 3. Desai, M. I. & Giacalone, J. Large gradual solar energetic particle events. *Living Reviews*
184 *in Solar Physics* 13, (2016).
- 185 4. Reames, D. V. Solar Energetic Particles: A Modern Primer on Understanding Sources.
186 Acceleration and Propagation, Lecture Notes in Physics 932 (Springer International
187 Publishing AG, 2017).
- 188 5. Cane, H. V., Richardson, I. G. & von Rosenvinge, T. T. A study of solar energetic
189 particle events of 1997–2006: Their composition and associations. *Journal of*
190 *Geophysical Research: Space Physics* 115, (2010).
- 191 6. Wibberenz, G. & Cane, H. V. Multi-Spacecraft Observations of Solar Flare Particles in
192 the Inner Heliosphere. *The Astrophysical Journal* 650, 1199-1207 (2006).
- 193 7. McComas, D. J. et al. Integrated Science Investigation of the Sun (ISIS): Design of the
194 energetic particle investigation. *Space Science Reviews* 204, 187-256 (2016).
- 195 8. Kasper, J. C. et al. Solar Wind Electrons Alphas and Protons (SWEAP) Investigation:
196 Design of the Solar Wind and Coronal Plasma Instrument Suite for Solar Probe Plus.
197 *Space Science Reviews* 204, 131-186 (2016).
- 198 9. Bale, S. D. et al. The FIELDS Instrument Suite for Solar Probe Plus. Measuring the
199 Coronal Plasma and Magnetic Field, Plasma Waves and Turbulence, and Radio
200 Signatures of Solar Transients. *Space Science Reviews* 204, 49-82 (2016).
- 201 10. Vourlidas, A. et al. The Wide-Field Imager for Solar Probe Plus (WISPR). *Space Science*
202 *Reviews* 204, 83-130 (2016).
- 203 11. Pizzo, V. A three-dimensional model of corotating streams in the solar wind, 1.
204 Theoretical foundations. *Journal of Geophysical Research* 83, 5563 (1978).
- 205 12. Gosling, J. Corotating and Transient Solar Wind Flows in Three Dimensions. *Annual*
206 *Review of Astronomy and Astrophysics* 34, 35-73 (1996).
- 207 13. Kasper, J. C. et al. *Nature*, (2019).

- 208 14. Bale, S. D. et al. *Nature*, (2019).
209 15. Kouloumvakos, A. et al. Connecting the Properties of Coronal Shock Waves with Those
210 of Solar Energetic Particles. *The Astrophysical Journal* 876, 80 (2019).
211 16. Chotoo, K. et al. The suprathermal seed population for corotating interaction region ions
212 at 1 AU deduced from composition and spectra of H⁺, He⁺⁺, and He⁺ observed on Wind.
213 *Journal of Geophysical Research: Space Physics* 105, 23107-23122 (2000).
214 17. Giacalone, J., Jokipii, J. R. & Kota, J. Particle Acceleration in Solar Wind Compression
215 Regions. *The Astrophysical Journal* 573, 845-850 (2002).
216 18. Zwickl, R. D., Roelof, E. C., Gold, R. E., Krimigis, S. M. & Armstrong, T. P. Z-rich solar
217 particle event characteristics 1972-1976. *The Astrophysical Journal* 225, 281 (1978).
218 19. Reinhard, R. & Wibberenz, G. Propagation of Flare Protons in the Solar Atmosphere.
219 *Solar Physics* 36, 473-494 (1974).
220 20. Kallenrode, M. B. Particle propagation in the inner heliosphere. *Journal of Geophysical*
221 *Research: Space Physics* 98, 19037-19047 (1993).
222 21. Richardson, I. G., von Rosenvinge, T. T. & Cane, H. V. The Properties of Solar
223 Energetic Particle Event-Associated Coronal Mass Ejections Reported in Different CME
224 Catalogs. *Solar Physics* 290, 1741-1759 (2015).
225 22. Widenbeck, M. E., et al., *The Astrophysical Journal*, Volume 762, Issue 1, article id. 54,
226 9 pp. (2013).
227 23. Bucik, R., et al. *ApJL* 869, L21 (2018), doi:10.3847/2041-8213/aaf37f
228 24. Bucik, R., et al., *The Astrophysical Journal*, May 2014, Volume 786, Issue 1, article id.
229 71, 12 pp doi:10.1088/0004-637X/786/1/71
230 25. Nitta, N., et al., *The Astrophysical Journal*, Volume 806, Issue 2, article id. 235, 12 pp.
231 (2015).

232

233 Sequential Figure Legends

234 Fig. 1: Orbit 1 and 2 Energetic Particle Summary Plot

235 Summary of observations of energetic particles (primarily H⁺) at lower energy (Lo: ~30-200
236 keV, inside orbital track) and higher energy (Hi: ~1-2 MeV, outside orbital track) from PSP's
237 first two orbits; intervals without data are indicated by the grey orbital track. Particle intensity is
238 indicated by both color and length of the bars. We identify Intervals **a-d** for detailed study.

239

240 Fig. 2: Recurring Corotating Energetic Particle Events

241 Corotating ion event seen in Intervals **a** (blue) and **b** (red) versus time (top) and as a function of
242 magnetic foot-point in Carrington longitude for a nominal 350 km s⁻¹ solar wind speed (bottom
243 panels).

244

245 Fig. 3: CME-Related Low-Energy Event and Following High-Energy Event

246 Time series (top five panels) of primarily protons at >1 MeV and ~30-500 keV, density and
247 radial speed¹³ and magnetic field vector and magnitude¹⁴ over Interval **c**. The bottom three
248 panels expand the dispersive SEP event and CME.

249

250 Fig. 4: Pair of Impulsive Events Near Second Perihelion

251 Two impulsive SEP events (Interval **d**) near PSP's second perihelion ($<40 R_{\odot}$) at higher energies
252 (top two panels) and lower energies (third and fourth panels), compared to the magnetic field
253 (bottom).

254

255 Extended Data Fig. 1: Viewing Geometry and Observation of Coronal Mass Ejection

256 Panel a: a view of the ecliptic plane from solar north at 14UT on 10 November 2018 showing the
257 relative positions of STEREO-A, Parker Solar Probe and dashed curves represent the orbits of
258 Mercury, Venus, and Earth. The field of view of the COR-2 instrument onboard STEREO-A is
259 shown as the red area. A CME off the East limb of the Sun as viewed from STEREO-A would be
260 roughly propagating towards Parker Solar Probe. This CME entered very gradually the field of
261 view of COR-2, part of the SECCHI suite of imaging instruments²⁶ aboard the Solar-Terrestrial
262 Relations Observatory (STEREO) spacecraft. Panel b: A running-difference image of the
263 Coronal Mass Ejection taken at 02:39UT on 11 November 2018 by COR-2A, extending in the
264 plane of the sky from 2 to 15 solar radii, provided images during the entire acceleration phase of
265 the CME. This CME entered COR-2A near 18UT on 10 November 2018 and transited through
266 the COR-2 field of view over ~12 hours.

267

268 Extended Data Fig. 2: Coronal Mass Ejection Model and Comparison to Magnetic Field Data

269 Panel a: the same as Fig. 1b but with superposed fitted-flux rope CME shape at 02:39UT on 11
270 November 2018 when the CME had passed half way through the COR-2A field of view. The
271 CME is very weak and no shock-sheath structure can be identified in these images. The typical
272 aspect of the CME in the image results from the line of sight integration of plasma distribution
273 on a bent toroid such that its major axis is located in a plane containing the observing spacecraft
274 (see very similar events in Thernisien et al. 2009²⁷, Rouillard et al. 2009²⁸). Panel b: The position
275 (red line) and speed (blue line) of the apex of the flux rope model was derived by comparing
276 iteratively each synthetic image produced by the 3-D model with each available COR-2A image.
277 A functional form (arctangent) was imposed for the flux rope's varying speed. The fitted CME
278 structure assumed in the present work is a bent toroid with an exponential increase of its cross-
279 sectional area from footpoint to apex as in Wood et al. (2009)²⁹. Panel b: The speed was derived
280 by fitting a hyperbolic tangent to the modeled CME position. The speed increases rapidly from
281 under 100 km/s at 18UT on 10 November to over 350 km/s when it exited the COR-2A field of
282 view at around 6UT on 11 November. Panel c: An internal magnetic field structure was
283 expressed analytically inside the envelope of the fitted CME (smooth curves) as in Isavnin
284 (2016),³⁰ but keeping here a simple circular cross section of the flux rope. By propagating this
285 flux rope at a constant speed of 380 km/s from the time it exits the COR-2 to Parker Solar Probe,
286 we predict an impact of the CME at PSP on 12 November 2018. The predicted arrival time and
287 the magnetic properties of the CME (thick smooth line) are in good agreement with those
288 measured in situ by the FIELDS (magnetic field data shown; thin lines) and SWEAP
289 instruments. We therefore conclude that the fitting procedure presented here provides a good
description of the CME evolution from the upper corona to PSP.

291

292 **Acknowledgements.** We are deeply indebted to everyone that helped make the PSP mission
293 possible. In particular, we thank all of the outstanding scientists, engineers, technicians, and
294 administrative support people across all of the ISOIS institutions that produced and supported the
295 ISOIS instrument suite and support its operations and the scientific analysis of its data. This
296 work was supported as a part of the PSP mission under contract NNN06AA01C. SDB
297 acknowledges the support of the Leverhulme Trust Visiting Professorship program and APR
298 acknowledges financial support from the ANR project COROSHOCK ANR-17-CE31-0006-01
299 and from the ERC project SLOW_SOURCE - DLV-819189.

300

301 **Author Contributions** D.J.M. is ISOIS PI and led the data analysis and writing of study. E.R.C
302 is ISOIS Deputy PI, helped develop EPI-Hi, and participated in the data analysis. C.M.S.C
303 helped develop EPI-Hi and participated in the data analysis. A.C.C. helped develop EPI-Hi and
304 participated in the data analysis. A.J.D. helped develop EPI-Hi and participated in the data
305 analysis. M.I.D. participated in the data analysis. J.G. participated in the data analysis. M.E.H
306 helped develop EPI-Lo and participated in the data analysis. C.J.J. produced Figures 3 and 4 and
307 participated in the data analysis. S.M.K. participated in the data analysis. A.W.L. helped develop
308 EPI-Hi and participated in the data analysis. R.A.L. helped develop EPI-Hi and participated in
309 the data analysis. O.M. participated in the data analysis. W.H.M participated in the data analysis.
310 R.L.M. led the development of EPI-Lo and participated in the data analysis. R.A.M helped
311 develop EPI-Hi and participated in the data analysis. D.G.M. helped develop EPI-Lo and
312 participated in the data analysis. A.P. participated in the data analysis. J.S.R. helped develop
313 EPI-Hi and participated in the data analysis. E.C.R. participated in the data analysis. N.A.S. led
314 the development of the ISOIS SOC and participated in the data analysis. E.C.S. helped develop
315 EPI-Hi and participated in the data analysis. J.R.S. led the development of the analysis tool,
316 produced Figures 1 and 2, and participated in the data analysis. M.E.W. led the development of
317 EPI-Hi and participated in the data analysis. S.D.B. is FIELDS PI and participated in the data
318 analysis. J.C.K. is SWEAP PI and participated in the data analysis. A.W.C. helped develop
319 SWEAP and participated in the data analysis. K.E.K. helped develop SWEAP and participated in
320 the data analysis. R.J.M. helped develop FIELDS and participated in the data analysis. M.P.
321 helped develop FIELDS and participated in the data analysis. M.L.S. helped develop SWEAP
322 and participated in the data analysis. A.P.R. led the CME simulation work and participated in the
323 data analysis.

324

325 **Author Information** Reprints and permissions information is available at
326 www.nature.com/reprints. The authors declare no competing financial interests. Readers are
327 welcome to comment on the online version of the paper. Publisher's note: Springer Nature
328 remains neutral with regard to jurisdictional claims in published maps and institutional
329 affiliations. Correspondence and requests for materials should be addressed to Dave McComas
330 (dmccomas@princeton.edu).

331

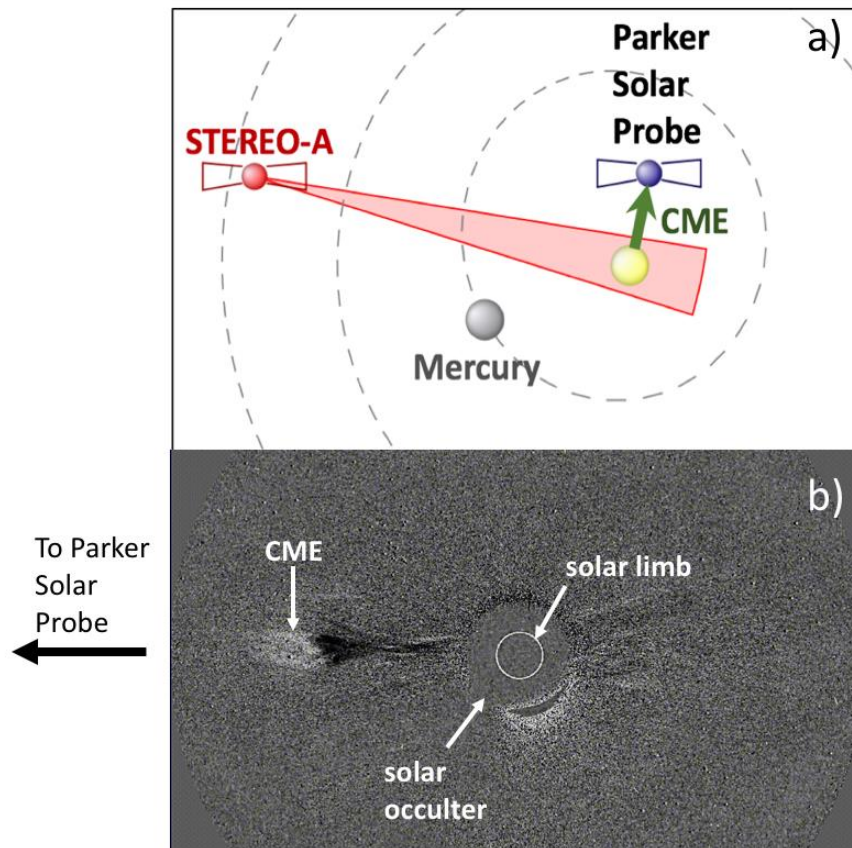
332 **Data Availability**

333 The PSP Science Data Management Plan, requires that all science data from the first two orbits
334 must be delivered to NASA's Space Physics Data Facility (SPDF) within six months of

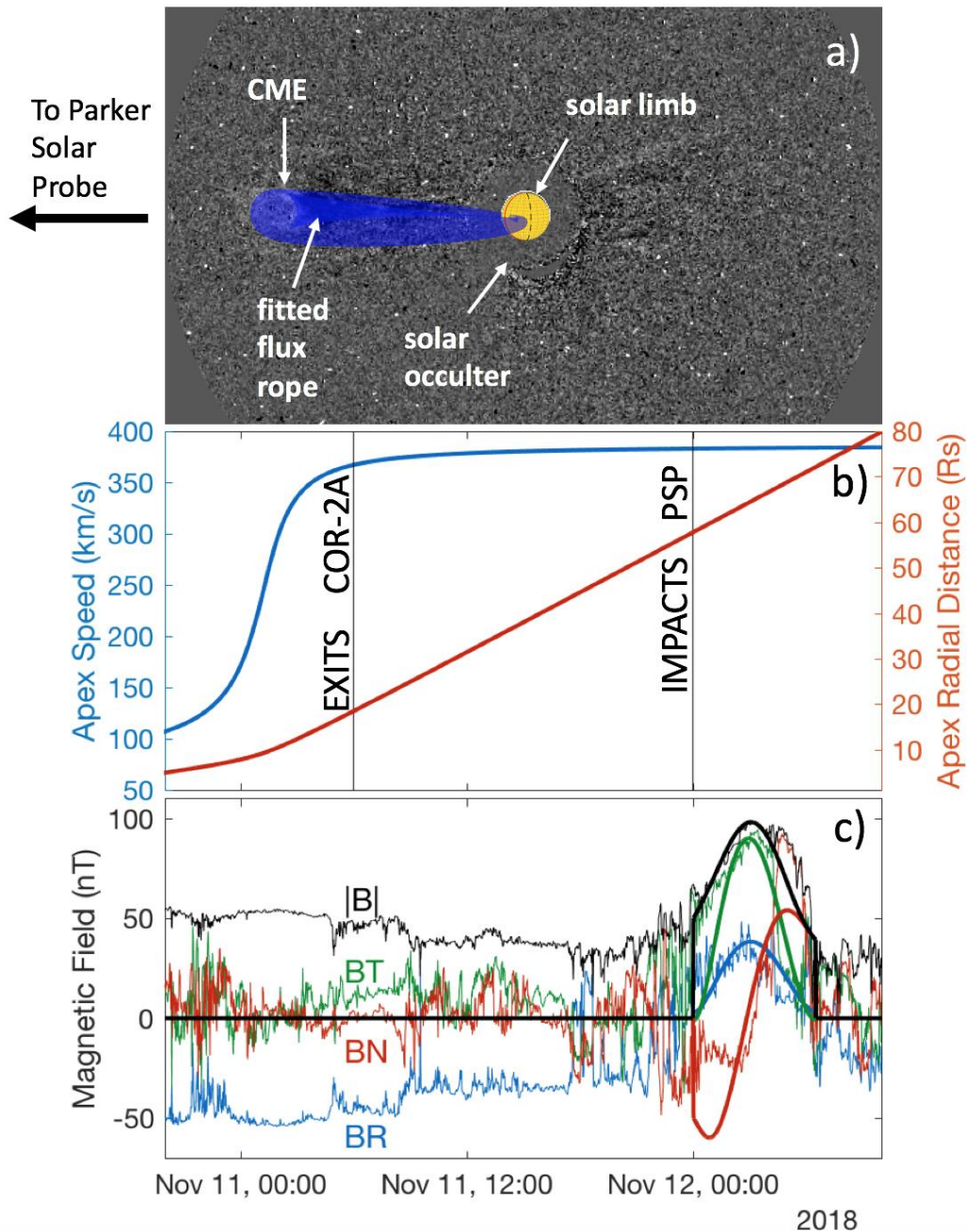
335 downlink. Thus, all data used in this study will be delivered to the SPDF no later than 12
336 November 2019 for public release.

337

338



340
 341 *Extended Data Fig. 1: Panel a: a view of the ecliptic plane from solar north at 14UT on 10*
 342 *November 2018 showing the relative positions of STEREO-A, Parker Solar Probe and dashed*
 343 *curves represent the orbits of Mercury, Venus, and Earth. The field of view of the COR-2*
 344 *instrument onboard STEREO-A is shown as the red area. A CME off the East limb of the Sun as*
 345 *viewed from STEREO-A would be roughly propagating towards Parker Solar Probe. This CME*
 346 *entered very gradually the field of view of COR-2, part of the SECCHI suite of imaging*
 347 *instruments²⁶ aboard the Solar-Terrestrial Relations Observatory (STEREO) spacecraft. Panel*
 348 *b: A running-difference image of the Coronal Mass Ejection taken at 02:39UT on 11 November*
 349 *2018 by COR-2A, extending in the plane of the sky from 2 to 15 solar radii, provided images*
 350 *during the entire acceleration phase of the CME. This CME entered COR-2A near 18UT on 10*
 351 *November 2018 and transited through the COR-2 field of view over ~12 hours.*



352

353 *Extended Data Fig. 2: Panel a: the same as Fig. 1b but with superposed fitted-flux rope CME*
 354 *shape at 02:39UT on 11 November 2018 when the CME had passed half way through the COR-*
 355 *2A field of view. The CME is very weak and no shock-sheath structure can be identified in these*
 356 *images. The typical aspect of the CME in the image results from the line of sight integration of*
 357 *plasma distribution on a bent toroid such that its major axis is located in a plane containing the*
 358 *observing spacecraft (see very similar events in Thernisien et al. 2009²⁷, Rouillard et al. 2009²⁸).*
 359 *Panel b: The position (red line) and speed (blue line) of the apex of the flux rope model was*
 360 *derived by comparing iteratively each synthetic image produced by the 3-D model with each*
 361 *available COR-2A image. A functional form (arctangent) was imposed for the flux rope's varying*
 362 *speed. The fitted CME structure assumed in the present work is a bent toroid with an exponential*

363 *increase of its cross-sectional area from footpoint to apex as in Wood et al. (2009)²⁹. Panel b:*
364 *The speed was derived by fitting a hyperbolic tangent to the modeled CME position. The speed*
365 *increases rapidly from under 100 km/s at 18UT on 10 November to over 350 km/s when it exited*
366 *the COR-2A field of view at around 6UT on 11 November. Panel c: An internal magnetic field*
367 *structure was expressed analytically inside the envelope of the fitted CME (smooth curves) as in*
368 *Isavnin (2016),³⁰ but keeping here a simple circular cross section of the flux rope. By*
369 *propagating this flux rope at a constant speed of 380 km/s from the time it exits the COR-2 to*
370 *Parker Solar Probe, we predict an impact of the CME at PSP on 12 November 2018. The*
371 *predicted arrival time and the magnetic properties of the CME (thick smooth line) are in good*
372 *agreement with those measured in situ by the FIELDS (magnetic field data shown; thin lines)*
373 *and SWEAP instruments. We therefore conclude that the fitting procedure presented here*
374 *provides a good description of the CME evolution from the upper corona to PSP.*

375

376 **Extended Data References**

377

- 378 26. Howard, R.A., Sun earth connection coronal and heliospheric investigation (SECCHI),
379 *Advances in Space Research*, 29, 12 (2002).
- 380 27. Thernisien, A., Vourlidas, A. & Howard, R. Forward Modeling of Coronal Mass Ejections
381 Using STEREO/SECCHI Data. *Solar Physics* 256, 111 (2009).
- 382 28. Rouillard, A.P. et al. A solar storm observed from the Sun to Venus using the STEREO,
383 Venus Express, and MESSENGER spacecraft. *Journal of Geophysical Research* 114,
384 (2010).
- 385 29. Wood, B. & Howard, R. An empirical reconstruction of the 2008 April 26 coronal mass
386 ejection. *The Astrophysical Journal* 702, 901–910 (2009).
- 387 30. Isavnin, A. FRiED: a novel three-dimensional model of coronal mass ejections. *The*
388 *Astrophysical Journal* 833, 2, 10 (2016).